Science of the Total Environment 826 (2022) 154103

Contents lists available at ScienceDirect

Science of the Total Environment

journal homepage: www.elsevier.com/locate/scitotenv

Deterioration of air quality associated with the 2020 US wildfires

Mikalai Filonchyk [a,b,*], Michael P. Peterson [c,**], Dongqi Sun [d,e,***]

[a] Faculty of Geomatics, Lanzhou Jiaotong University, Lanzhou 730070, China
[b] Gansu Provincial Engineering Laboratory for National Geographic State Monitoring, Lanzhou 730070, China
[c] Department of Geography/Geology, University of Nebraska Omaha, Omaha, NE 68182, USA
[d] Institute of Geographic Sciences and Natural Resources Research, CAS, Beijing 100101, China
[e] Key Laboratory of Urban Land Resources Monitoring and Simulation, Ministry of Natural Resources, Shenzhen 518034,China

HIGHLIGHTS

- Multi-satellite observation of wildfires
- Spatial and temporal variations of $PM_{2.5}$ were analyzed.
- AOD and UVAI exceeded 1 and 2 over most of the country.
- The hardest hit by wildfires are California, Oregon, and Washington.

GRAPHICAL ABSTRACT

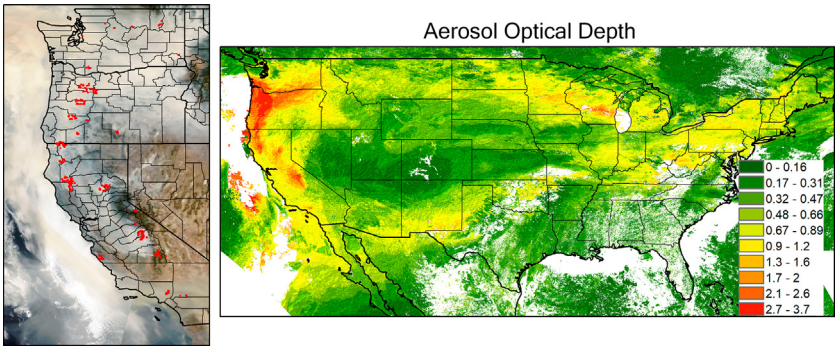

ARTICLE INFO

Article history:
Received 2 October 2021
Received in revised form 28 January 2022
Accepted 19 February 2022
Available online 24 February 2022

Editor: Pavlos Kassomenos

Keywords:
Wildfires
United States
$PM_{2.5}$
Aerosol optical depth
Ultraviolet aerosol index
MAIAC
TROPOMI

ABSTRACT

The wildfires of August and September 2020 in the western part of the United States were characterized by an unparalleled duration and wide geographical coverage. A particular consequence of massive wildfires includes serious health effects due to short and long-term exposure to poor air quality. Using a variety of data sources including aerosol optical depth (AOD) and ultraviolet aerosol index (UVAI), obtained with the Moderate-Resolution Imaging Spectroradiometer (MODIS), Multi-Angle Implementation of Atmospheric Correction (MAIAC) and Tropospheric Monitoring Instrument (TROPOMI), combined with meteorological information from the European Center for Medium-Range Weather Forecasts (ECMWF) and other supporting data, the impact of wildfires on air quality is examined in the three western US states, California, Oregon, and Washington, and areas to the east. The results show that smoke aerosols not only led to a significant deterioration in air quality in these states but also affected all other states, Canada, and surrounding ocean areas. The wildfires increased the average daily surface concentration of $PM_{2.5}$ posing significant health risks, especially for vulnerable populations. Large amounts of black carbon (BC) aerosols were emitted into the atmosphere. AOD and UVAI exceeded 1 and 2 over most of the country. In parts of the three western states, those values reached 3.7 and 6.6, respectively. Moreover, a reanalysis based on MERRA-2 (Modern-Era Retrospective Analysis for Research and Applications, version 2) showed that the maximum values of BC surface mass concentration during the wildfires were about 370 $\mu g/m^3$. These various indicators provide a better understanding of the extent of environmental and atmospheric degradation associated with these forest fires.

* Correspondence to: M. Filonchyk, Faculty of Geomatics, Lanzhou Jiaotong University, Lanzhou 730070, China.
** Correspondence to: M.P. Peterson, Department of Geography/Geology, University of Nebraska Omaha, Omaha, NE 68182, USA.
*** Correspondence to: D. Sun, Institute of Geographic Sciences and Natural Resources Research, CAS, Beijing 100101, China.
E-mail addresses: filonchyk.mikalai@gmail.com (M. Filonchyk), mpeterson@unomaha.edu (M.P. Peterson), sundq@igsnrr.ac.cn (D. Sun).

http://dx.doi.org/10.1016/j.scitotenv.2022.154103

1. Introduction

Biomass combustion is the main global source of fine carbonaceous aerosols in the form of black carbon (BC) and organic carbon (OC) (Smirnov et al., 2015). Biomass aerosols are mainly generated by man-made fires such as the burning of crops, deforestation and the burning of biofuels, as well as wildfires. Wildfires not only emit large amounts of greenhouse gases (Tian et al., 2011; Wotton et al., 2017) but they have a significant effect on the optical and microphysical characteristics of clouds (Martins and Dias, 2009; Liu et al., 2013; Meyer et al., 2015), the processes of sedimentation (Avissar et al., 2002; Dias et al., 2002; Khain et al., 2008; Leng et al., 2014), increase the scale of carbon-containing emissions causing changes in the state of climatically-active components of the atmospheric layer (Rakhimov et al., 2014), alter surface reflectivity leading to variations in radiative forcing (Huang et al., 2016), and severely damage the functioning of forest ecosystems (Jiang and Zhuang, 2011; Wang et al., 2012; Nikhil et al., 2021; Zhou et al., 2021a). Of most direct and immediate concern for humans is the deterioration of air quality and the accompanying damage to human health.

Atmospheric aerosols, also known as particulate matter, and its constituents $PM_{2.5}$ (particulates with diameters ≤ 2.5 μm) and BC, are radiation-active components of the atmosphere (Gustafsson and Ramanathan, 2016; Akinwumiju et al., 2021; Mozny et al., 2021; Zhou et al., 2021b). BC is a byproduct of combustion and has a significant effect on the atmosphere, settling on low-lying clouds and trapping the heat on the Earth's surface. Estimates of the variability of the relative contents of BC and $PM_{2.5}$ in atmospheric aerosols are important for the modernization of both empirical aerosol models and climatic estimates (Westervelt et al., 2016; Chen et al., 2018). In addition, due to air currents, aerosols travel long distances and can have a major effect on air quality even far from its source.

The United States is currently one of the world leaders for both the number of wildfires recorded annually and the affected areas. The states of California, Oregon, and Washington are some of the most flammable in terms of wildfires, despite constant improvement in the means and methods for preventing, early detection, and fighting both the wildfires themselves and their consequences. As a result of increased drought, the problem of wildfires in California has become especially urgent in recent years (Raffuse et al., 2013; Louie, 2020; Li et al., 2020a,b). The main problem of limiting wildfires over huge areas is the difficulty of detecting them in time, especially with sparse populations. A variety of satellite imagery is used to detect and monitor wildfires (Gorchakov et al., 2014; Shikwambana, 2019; Zhu et al., 2019; Nguyen et al., 2021; Zhang et al., 2021). These same satellites and others can be used to monitor resultant air quality over a large area.

During the COVID-19 pandemic, air quality improved in many parts of the world as flights, road traffic, and factory emissions were reduced (Filonchyk and Peterson, 2020; Kumari and Toshniwal, 2020; Menut et al., 2020; Wyche et al., 2021; Zhu et al., 2020; Naqvi et al., 2021). At the same time, high levels of air pollution caused by forest fires were observed in some parts of the world. However, in mid-August 2020, unfavorable climatic and natural factors on the west coast of the United States (Fig. S1) led to the outbreak of wildfires. Smog, from relentless forest fires in the western states, spread across the country affecting air quality even in the eastern parts of the continent.

By September 12, 2020, over 100 wildfires raged in the states of Oregon, California, and Washington. The total affected area was almost 2 million hectares (nearly 5 million acres). More than 1.3 million hectares (3,212,370 acres) of land burned. By the end of 2020, nearly 1.8 million hectares (4,447,897 acres) were burned in California alone. The wildfires destroyed more than 10,000 buildings and caused more than $12 billion in damage, including over $10 billion in property damage and over $2 billion in firefighting costs (Louie, 2020). The California wildfires in 2020 are the largest recorded wildfires in modern history (Keeley and Syphard, 2021).

The combined use of ground and satellite observations, along with meteorological data, can result in a better understanding of the spatial and temporal characteristics of aerosols. In this paper, we examine aerosols in the atmosphere using data products from Tropospheric Monitoring Instrument (TROPOMI) and Moderate Resolution Imaging Spectroradiometer (MODIS), combined with meteorological data from the European Center for Medium-Range Weather Forecasts (ECMWF), as well as $PM_{2.5}$ readings from ground monitoring stations in the period from 10 to 16 September 2020. The results of this study provide a better understanding of the deterioration of air quality as a result of the fires. The multifaceted approach provides a model for how air pollution from forest fires can be examined.

2. Data sources and methodology

To gain a better perspective on the 2020 forest fires across the United States, a variety of satellite and ground-based data are used in this study. The purpose is to better understand how the deterioration of air quality from forest fires can be detected with a variety of data sources. We begin by examining the sources of data.

2.1. $PM_{2.5}$ measurements

$PM_{2.5}$ are fine inhalable particles with diameters generally 2.5 μm and smaller. By getting deep into lungs, these fine particles pose the greatest health risk. Some of these particles even get into the bloodstream. Daily $PM_{2.5}$ concentrations (measured in $\mu g/m^3$) for the studied area were obtained through 24-h daily sampling from the US Environmental Protection Agency (EPA). Average daily values in the period from August 15 to September 25, 2020 were downloaded from the EPA's Air Quality System. $PM_{2.5}$ data were obtained from 336 monitoring stations located in different parts of the country, including both rural and urban areas.

2.2. MAIAC AOD data

Data on aerosol optical depth (AOD) were interpolated from the Multi-Angle Implementation of Atmospheric Correction (MAIAC). MAIAC performs atmospheric correction using a method developed for the Moderate Resolution Imaging Spectroradiometer (MODIS) (Lyapustin et al., 2018). Time series analysis and spatial processing is used to separate the contributions of the atmosphere and surface to improve cloud detection as well as aerosol and surface characteristics. The process performs well for both dark surfaces covered with vegetation and bright ones in the desert. The algorithm results in a spatial resolution of 1 km making it possible to conduct research on a local scale. To analyze the spatial and temporal distribution of aerosols during the wildfires, MODIS-MAIAC Land Aerosol Optical Depth (AOD) Daily Level 2 product (MCD19A2) at a wavelength of 550 nm was obtained from NASA's Earth Observing System Data.

2.3. TROPOMI

Launched in 2017 by the European Space Agency (ESA), the Sentinel-5 Precursor satellite was designed for the daily global atmospheric observation of the Earth's chemical composition, including the content and distribution of major pollutants and greenhouse gases. Its main sensor is the Tropospheric Monitoring Instrument (TROPOMI), collecting data in the ultraviolet, visible, near, and mid-infrared ranges (Veefkind et al., 2012). The spatial resolution of the sensor is 5.5×3.5 km. The sensor has global coverage with a 24-h temporal resolution. TROPOMI records the reflectivity of wavelengths interacting with various constituents of the atmosphere, including aerosols, NO_2 (nitrogen dioxide), O_3 (ozone), SO_2 (sulfur dioxide), CO (carbon monoxide), HCHO (formaldehyde), and the important greenhouse gas, CH_4 (methane).

The Ultraviolet Aerosol Index (UVAI) is based on spectral contrast in the ultraviolet (UV) spectral range for pairs of wavelengths at 340 and 380 nm, where the difference between the observed and modeled reflectivity gives the residual value. If this value is positive, it indicates the presence of UV-absorbing aerosols such as dust and smoke. Clouds produce residual values close to zero, and negative residual values may indicate the presence of

non-absorbing aerosols. This index is ideal for tracking the evolution of episodic aerosol plumes from dust flares, volcanic ash, and biomass burning. TROPOMI Level 2 UVAI data were downloaded from the Copernicus Open Access Hub platform.

2.4. MERRA-2

The Modern-Era Retrospective Analysis for Research and Applications, version 2 (MERRA-2), was developed at NASA's Global Modeling and Assimilation Office (GMAO). MERRA-2 reanalysis is based on the GEOS-5 model (Goddard Earth Observing System, version 5.12.4), containing blocks of information for modeling atmospheric and ocean circulation, atmospheric composition, biogeochemistry, processes on the Earth's surface collected over the satellite's operational era (from 1980 to present) (Gelaro et al., 2017). The model has 72 levels from the surface to 0.01 hPa with a spatial resolution of 0.5 × 0.625°. MERRA-2 reanalysis includes the assimilation of aerosol observational data based on GEOS-5, integrated with GOddard Chemistry Aerosol, Radiation and Transport (GOCART), providing information on five atmospheric aerosols: sea salt, dust, OC and BC, and sulfate aerosols. The GEOS-5 model also includes the assimilation of aerosol optical depth (AOD) from satellite observations using MODIS, AVHHR and MISR, as well as ground-based measurements from the AERONET network. The MERRA-2 information product is divided into dozens of subsets according to parameters, sizes, and spatial-temporal resolution. This study used BC surface mass concentration (BCSMASS) in the MERRA-2 subset M2T1NXAER (or tavg1_2d_aer_Nx) downloaded from NASA's Goddard Earth Sciences Data and Information Services Center (GES DISC).

2.5. CAMS

The Copernicus Atmosphere Monitoring Service (CAMS) global forecasting system, implemented by the European Center for Medium-Range Weather Forecasts (ECMWF), monitors the daily activity of wildfires around the world based on satellite observations. It monitors their intensity and estimated emissions and allows CAMS to build a more long-term pattern of fire activity. CAMS enables wildfire observations with NASA's Terra MODIS and Aqua MODIS instruments in its Global Fire Assimilation System (GFAS). GFAS assimilates fire radiative power (FRP) observation from satellite sensors to provide daily estimates of emissions from wildfires and biomass burning. This parameter estimates the amount of thermal energy released per unit of time during the burning of vegetation (Li et al., 2020a).

In this study, we used a technique for calculating the FRP index that makes it possible to estimate the integral radiation power of heat radiation from a thermally active zone, an indicator of the contribution to air pollution. Wooster et al. (2005) showed a linear relationship between FRP and combustion intensity, verifying that the higher the FRP value, the higher the biomass combustion rate. More burning biomass results in more smoke entering the atmosphere that can be transported over considerable distances from the fire site. The spatial resolution of GFAS data is 0.1°. GFAS fire data is based on satellite observations of active wildfires but the system tries to minimize the detection of other heat sources such as volcanoes and gas flares that would limit its applicability to wildfires.

2.6. FIRMS

The Fire Information for Resource Management System (FIRMS) was developed at the University of Maryland and supported by the National Aeronautics and Space Administration (NASA). The system allows you to receive operational information about the location of hot spots in real-time within 3 h after the MODIS (Moderate Resolution Imaging Spectroradiometer) satellite has passed. According to MODIS data, a wildfire is detected when a temperature anomaly is recorded over the area under study. According to the MODIS satellite probe, thermal anomalies represent the center of a 1 km pixel, which was marked by the MOD14/MYD14 Fire and Thermal Anomalies (Justice et al., 2002). MODIS temporal resolution is 1–2 days.

2.7. CALIPSO

CALIPSO (Cloud-Aerosol Lidar and Infrared Pathfinder Satellite Observation) is a US-French research satellite launched as part of NASA's Earth Observing System (EOS). It is designed to study the Earth's cloud coverage. The main purpose of CALIPSO is to carry out global measurements of aerosols and clouds. Such measurements are necessary to study the degree to which aerosols and clouds influence the climate system. Satellite lidar height-distributed backscatter measurements are independent of surface reflection and require an aerosol extinction-to-backscatter ratio. The aerosol ratio is calculated by comparing wavelengths of 532 and 1064 nm, defining the types of aerosols, such as dust, polluted continental, clean marine, clean continental, polluted dust and smoke (from wildfires). The CALIPSO satellite data was analyzed to determine the type of aerosols over the study region during the period of wildfires. CALIPSO Level 2 Vertical Feature Mask (VFM) and Level 2 Aerosol Profile version 4–21 data product was used with a horizontal grid of 5 km and a vertical resolution of 30 m (for heights below 8.2 km). The data has been filtered for quality purposes. For this, only cloudless profiles were used. The CALIPSO cloud and aerosol detection score provides a numerical confidence level for classifying layers using the CALIOP cloud-aerosol discrimination (CAD) algorithm. CAD scores range from −100 to 100, with negative values indicating aerosols and positive values indicating clouds. The larger the CAD scores, the higher the confidence in the correctness of the classification. The CAD score was required to be between −100 and −70 (Liu et al., 2010).

2.8. Meteorological data

Meteorological data used in this study included air temperature at a height of 2 m above ground, wind speed and wind vectors at 10 m above ground, surface pressure, and relative humidity at 850 hPa. All meteorological data were obtained from the ERA5 reanalysis data provided by the European Center for Medium-Range Weather Forecasts (ECMWF). The spatial resolution is 0.25 × 0.25°, with atmospheric parameters on 37 pressure levels (ECMWF, 2018).

3. Results

3.1. Analysis of ground-based $PM_{2.5}$ concentrations

During the wildfires, air quality in the area of the wildfires plummeted and reached the level of the most polluted cities in the world. As a result of the spread of fire over thousands of square kilometers, a record amount of soot and other combustion products were released into the atmosphere. This turned the skies in the US west to a red and orange color (CBS, 2020).

Although the wildfires began in mid-August, the greatest impact on air quality came a month later, in mid-September. The level of pollution in some regions of the country increased four to eleven times above the 35 μg/m^3 for $PM_{2.5}$ National Ambient Air Quality Standards (NAAQS) limit set by the United States Environmental Protection Agency. Thus, according to Fig. 1, from September 10 to September 16, 2020, concentrations of $PM_{2.5}$ exceeding 150 μg/m^3 were recorded in the largest cities of California, Oregon, and Washington such as San Francisco, Los Angeles, Seattle, Tacoma, Kent, Fresno and Oakland. In some cities, including Beaverton, Medford, Spokane, and Corvallis, these numbers were over 250 μg/m^3. In the Oregon cities of Portland, Salem, Eugene and Springfield along with of Vancouver, Washington, it was over 400 μg/m^3. In terms of air quality, these cities briefly became some of the most polluted in the world, with pollution values higher than even the largest cities in India, China, Pakistan, and Bangladesh including Delhi, Kanpur, Beijing, Tianjin, Lahore, and Dhaka.

Wildfires resulted in the release of hazardous air pollutants such as BC and OC, as well as gaseous aerosol precursors, that further contribute to

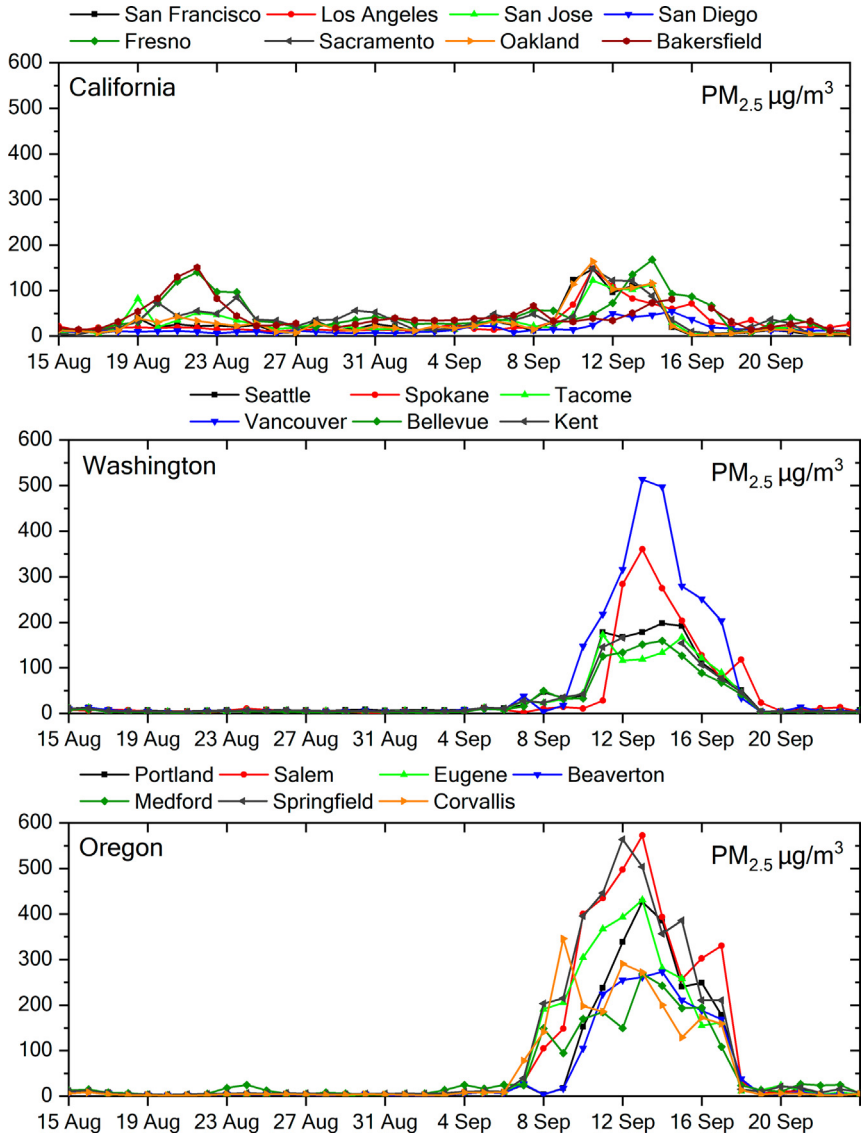

Fig. 1. Average daily $PM_{2.5}$ concentration in major cities in California, Washington, and Oregon from August 15 to September 25, 2020.

higher $PM_{2.5}$ values. Data from 336 $PM_{2.5}$ monitoring stations were interpolated using the inverse distance weighted (IDW) technique to create the map in Fig. 2. The map depicts the western part of the US during the most severe wildfires. In mid-September, smoke from numerous wildfires covered most of the states of Oregon and Washington, as well as northern and eastern California. According to Fig. 2, the most affected counties were Mono (CA), Klickitat (WA), Deschutes (OR), Josephine (OR), Lane (OR), Linn (OR), and Marion (OR) where the average daily $PM_{2.5}$ concentration during the week from 10 to 16 March exceeded 350 µg/m^3. (More details on the location of counties are provided in Fig. S2 of the Supplementary Materials.)

The Fire Information for Resource Management System (FIRMS) was used to identify wildfire hotspots. According to the obtained data, in the United States during the study period of 2020, a total of 35,346 fire spots (confidence level > 80%) were registered, nearly 7 times more than the 4479 in 2019. The distribution of the fire counts within the study area is represented in Fig. 3. The Kernel Density algorithm was used to identify several large wildfires represented by clustered fire counts. It can be noted that most of the wildfires were in California, Washington, and Oregon, accounting for over 85% of all wildfires reported in the entire country in 2020.

3.2. Fire radiative power and $PM_{2.5}$ fluxes derived from the CAMS

Fig. 4 shows the distribution of wildfire radiative power, in the range between 0.01 and 32 W m^{-2}, similar to the wildfires shown in Fig. 3. Several studies using small experimental wildfires have demonstrated that the total amount of FRP released during a fire has a simple linear relationship with the total amount of biomass fuel consumed (Wooster et al., 2005; Freeborn et al., 2008; Mota and Wooster, 2018). It is worth noting that high FRP values are consistent with high values of $PM_{2.5}$ as measured by ground stations (see Fig. 2).

The quantification of aerosol fluxes is vital to improving the fundamental understanding of the Earth system in the face of multiple biogeochemical changes. Data on $PM_{2.5}$ fluxes are critical to understanding their emission pathways. $PM_{2.5}$ fluxes provided by GFAS (Fig. 4) also indicates the source of emissions — the combustion of biomass (forest vegetation or shrubs). Fig. 4 shows the estimated $PM_{2.5}$ fluxes. Pollutant emissions have been localized and associated with high $PM_{2.5}$ concentrations and high FRP values. At the sites with the highest emissions, $PM_{2.5}$ fluxes exceeded 300 µg m^{-2} s^{-1}. The original map presumably reflects emission sources associated with intense fires. This is not surprising since the burning of fossil fuels is one of the main sources of $PM_{2.5}$.

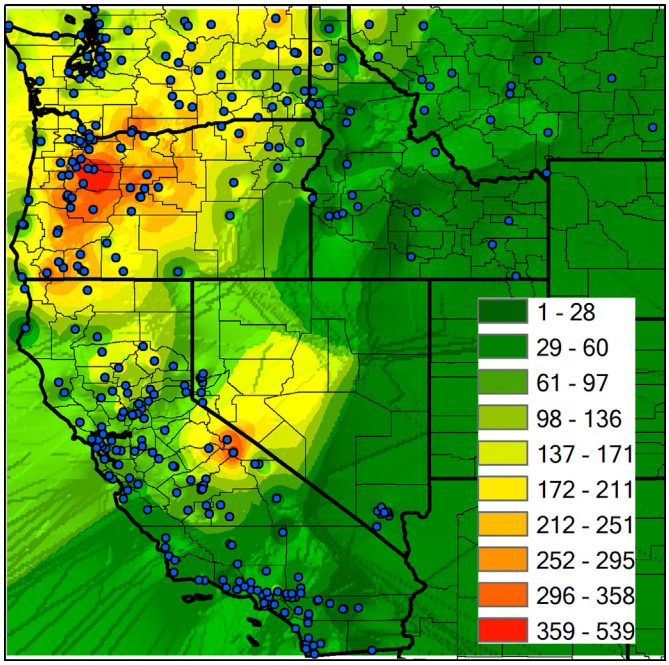

Fig. 2. Spatial distribution of $PM_{2.5}$ (in μg/m^3) in the western US from 10 to 16 September 2020. 24-h mean values above 25 μg/m^3 are considered dangerous to human health (World Health Organization (WHO), 2005).

The combustion of biomass is one of the main problems faced in all regions of the world. In addition to protecting biodiversity, forests perform ecosystem functions crucial to agriculture, including regulating the water and carbon cycles. Climate change, accompanied by an overall decrease in precipitation in the western US, leads to a decrease in the number of extinguished wildfires, resulting in the release of a large amount of soot into the upper atmosphere. The problem is further escalated by the fact that these particles appear in the central and eastern parts of the country, affecting changes in the rainfall cycle in these regions.

Precipitation is another factor associated with aerosols in the atmosphere. A number of studies have shown that a large amount of emissions of particulate matter formed as a result of wildfires lead to a change in the mechanisms of cloud formation and their growth, as well as the nature of precipitation. This prevents the formation of small clouds, delaying or even restraining precipitation over large areas affected by fire emissions (Avissar et al., 2002; Dias et al., 2002) thus limiting the air cleansing potential of precipitation.

Aerosol particles often can act as cloud condensation nuclei (CCN), on the surfaces of which water vapor can thicken and condense in the air. If the environment is relatively clean, then CCNs are few. The ability of these particles to form cloud droplets differs depending on their size as well as their exact composition since the hygroscopic properties of these various components are very different. Particulate sulfates and sea salt that easily absorb water can act as CCN, growing rapidly, colliding with smaller particles and fall out as rain. If the atmosphere is contaminated with large amounts of insoluble CCN particles such as soot or BC from wildfires, water droplets will grow slowly as the cloud grows (Khain et al., 2008; Leng et al., 2014). Often these clouds don't produce rain as the droplets evaporate before reaching a critical size for precipitation, and water droplets, together with aerosols, do not return to the ground but are carried away by wind.

3.3. Characteristics of aerosol properties

The wildfires in the western United States resulted in large concentrations of pyrogenic carbon released into the atmosphere, with extremely dense and extensive plumes of smoke that could be observed from space. In addition to ground-based monitoring data, satellite data were used to determine aerosol loading and the transport of pollutants. Spatial gaps in ground-based monitoring are inevitable, and satellite data can fill air quality information in areas where ground-based monitoring is not available. The choice of satellite data to address specific air quality problems depends, in part, on data accuracy and spatial and temporal resolution.

Satellite data were sampled September 10–16 when the maximum number of wildfires were observed. This was also the time-frame with the highest concentrations of $PM_{2.5}$ for the entire observation period beginning when forest fires first started at the beginning of August. Intense heat and drought that sparked catastrophic wildfires in the west of the US were intensified by strong winds. Many satellites and other space instruments closely monitor the development of these wildfires. According to the FIRMS data, over 8000 hot spots were registered in the period from 10 to 16 September in three states: California, Oregon, and Washington (Fig. 5).

True-color MODIS/Terra images show that a huge area has been affected by heavy smoke from fires. As shown in Fig. 5, the MODIS image shows the presence of aerosol plumes from wildfires covering most of the west of the country, including adjacent ocean areas. Fire spots are marked with red dots and thick smoke from fires is evident with gray plumes. Note that the wildfires correspond to the spatial distribution of flux of

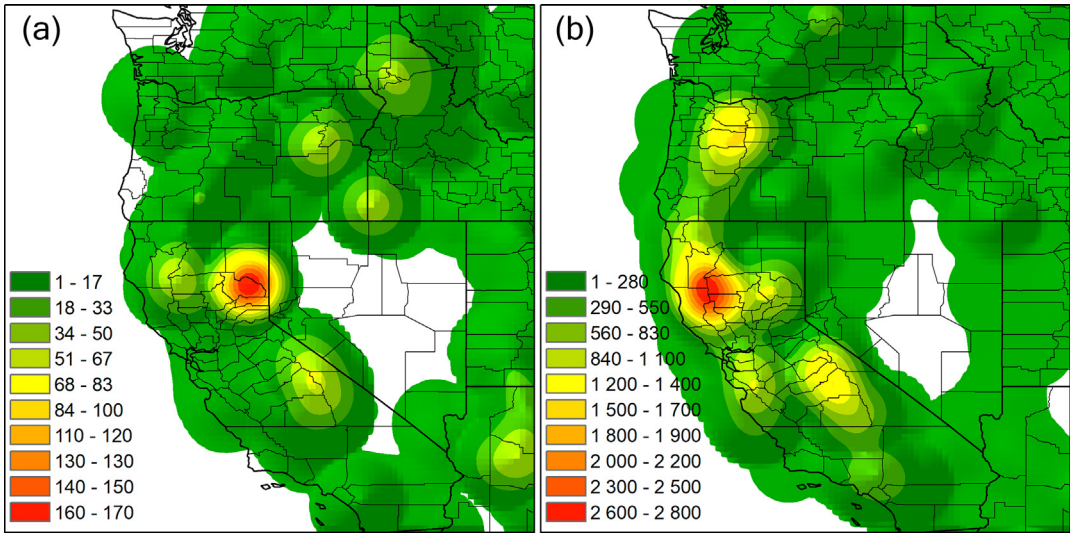

Fig. 3. Kernel density map of the hot spots observed from FIRMS data over the west coast of the US between August 16 and September 25, 2019 (a) and 2020 (b).

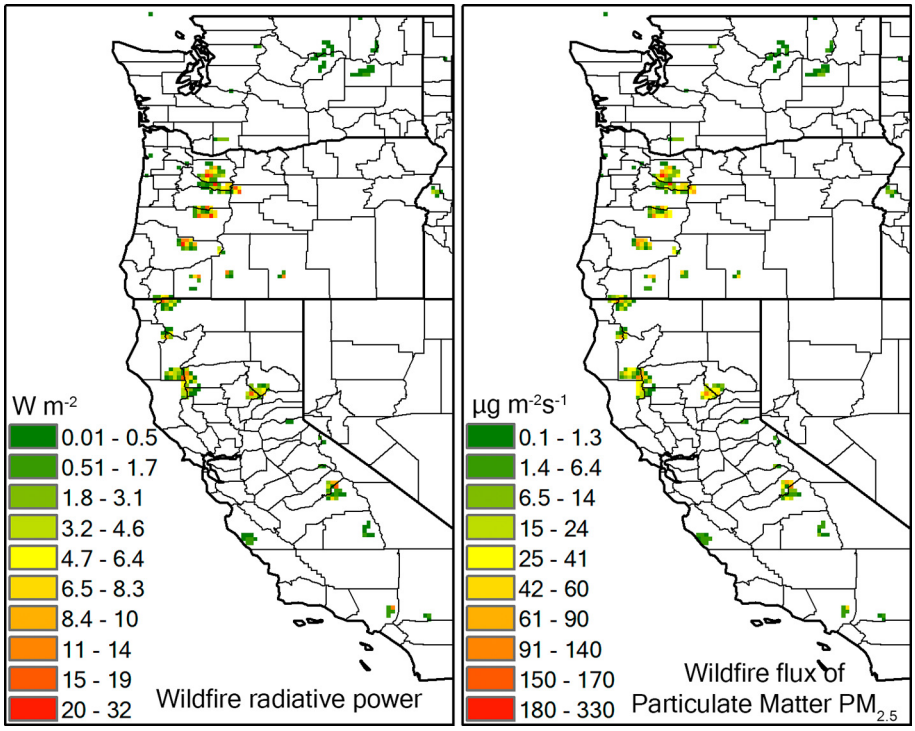

Fig. 4. Wildfire radiative power (in W m^{-2}) and wildfire flux of particulate matter $PM_{2.5}$ (in µg m^{-2} s^{-1}) derived from the CAMS Global Fire Assimilation System from 10 to 16 September 2020.

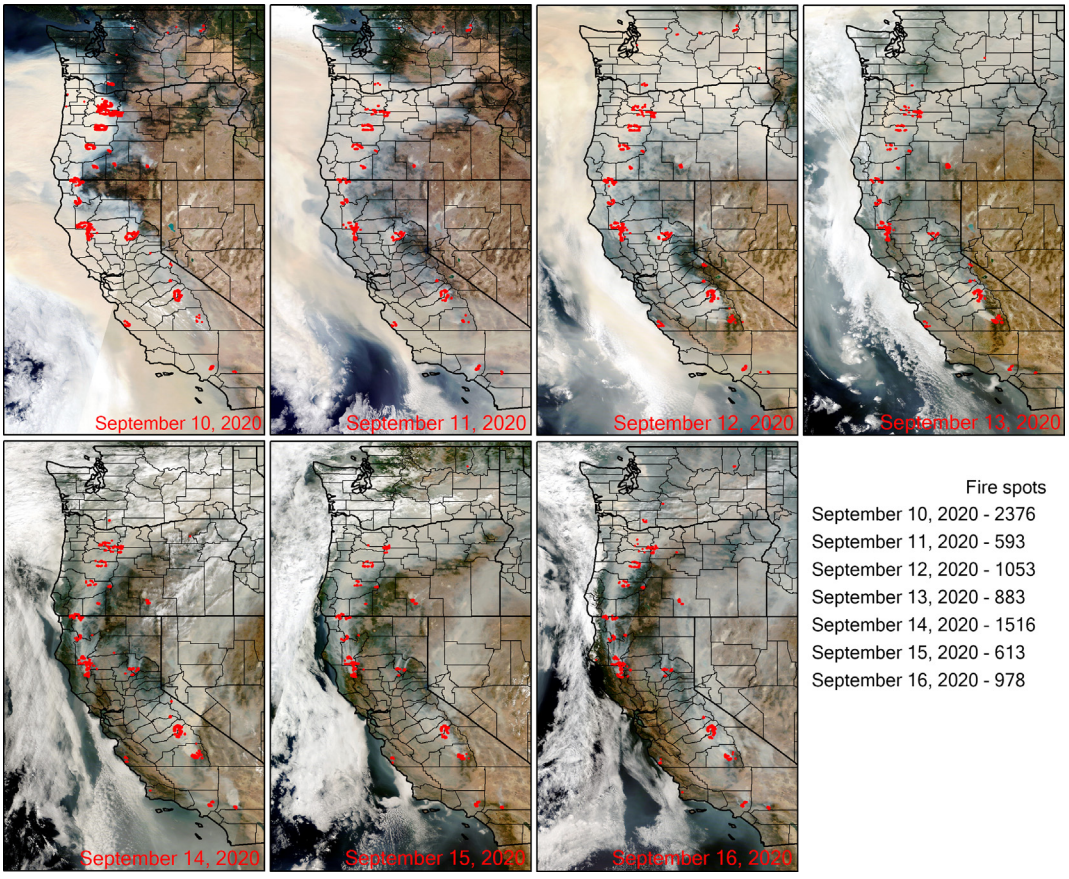

Fig. 5. MODIS/Terra true-color image with super-imposed FIRMS fire spots in the period from 10 to 16 September 2020. The red dots indicate areas of active fire.

CAMS $PM_{2.5}$ in Fig. 4. This confirms that smoke aerosols were formed as a result of wildfires, and not another phenomenon.

An important indicator of smoke thickness is aerosol optical depth (AOD), obtained from MODIS MAIAC, and ultraviolet aerosol index (UVAI), obtained from TROPOMI. AOD is a measure of light extinction (absorption + scattering) caused by atmospheric aerosols. High AOD values, greater than 0.6, indicate the presence of more aerosols and suspended particles in the atmosphere and therefore a significant amount of absorption and scattering of radiation, while lower AOD values indicate fewer aerosols and increased transmission of radiation. UVAI indicates the presence of UV-absorbing aerosols in the atmosphere, like dust and smoke. If the UVAI values are positive, it indicates absorbing aerosols (dust and smoke). If small or negative, it indicates non-absorbing aerosols or clouds. Therefore, these parameters can be used as monitoring indicators for the state of the atmosphere.

Biomass combustion in a wildfire can result in the release of large quantities of smoke aerosols. The daily frequency and global coverage of measurements from MODIS and TPOPOMI satellite instruments allow tracking the transport of such an aerosol plume over days and even weeks. Fig. 6 show the circulation of aerosols caused by the massive wildfires that ultimately affected air quality in the northern, southern, and eastern states.

AOD and UVAI data from September 10–16 were selected to analyze the local impacts of carbonaceous aerosols emitted from severe wildfires and their further impact on air quality in other regions. During this period, a large amount of BC aerosols were detected with AOD and UVAI values in most of the territory during this period exceeding 1 and 2, respectively. Higher values of AOD and UVAI indicate the presence of a large amount of aerosols in the atmospheric column. This significantly degraded air quality, especially in California, Oregon, and Washington, where values of AOD and UVAI in some areas reached 3.7 and 6.6, respectively. Areas with high values of AOD and UVAI coincide with wildfires and smoke shown in Fig. 5 and also coincide with high concentrations of $PM_{2.5}$ shown in Figs. 2 and 4. According to the spatial distribution of UVAI shown in Fig. 6b, the smoke cloud has spread not only eastward, but also westward above the Pacific Ocean. Strong winds blew smoke thousands of kilometers to major cities on the country's east coast, including New York, Washington, Boston, Philadelphia, Baltimore and Portland (ME), which is also confirmed by previous studies (Hung et al., 2021). The higher elevations found in Colorado, Utah and Wyoming in the west central US limited the transport of aerosols. Although closer to the fires, these states had lower AOD and UVAI values.

ABL is the lowest part of the troposphere and has an important impact on the atmospheric environment. Concentrations of air pollutants emitted from various anthropogenic activities or biomass burning are concentrated in the ABL. The height of the air mass plays an important role in the life cycle of smog, especially when the air mass interacts with the atmospheric boundary layer (ABL), and affects the heating and dynamics of the atmosphere, deposition and PM concentration at the surface. The height of the ABL indicates the degree of turbulence and dispersion of air pollutants (Uzan et al., 2016). Ground air pollutant concentrations at higher ABL are lower than at lower ABL (Kawai et al., 2018.).

ABL heights over the western and central US from ECMWF ERA5 reanalysis are shown in Fig. S3. The reanalysis data show that the height of the ABL above the study area ranged from 500 m to over 3000 m, which may

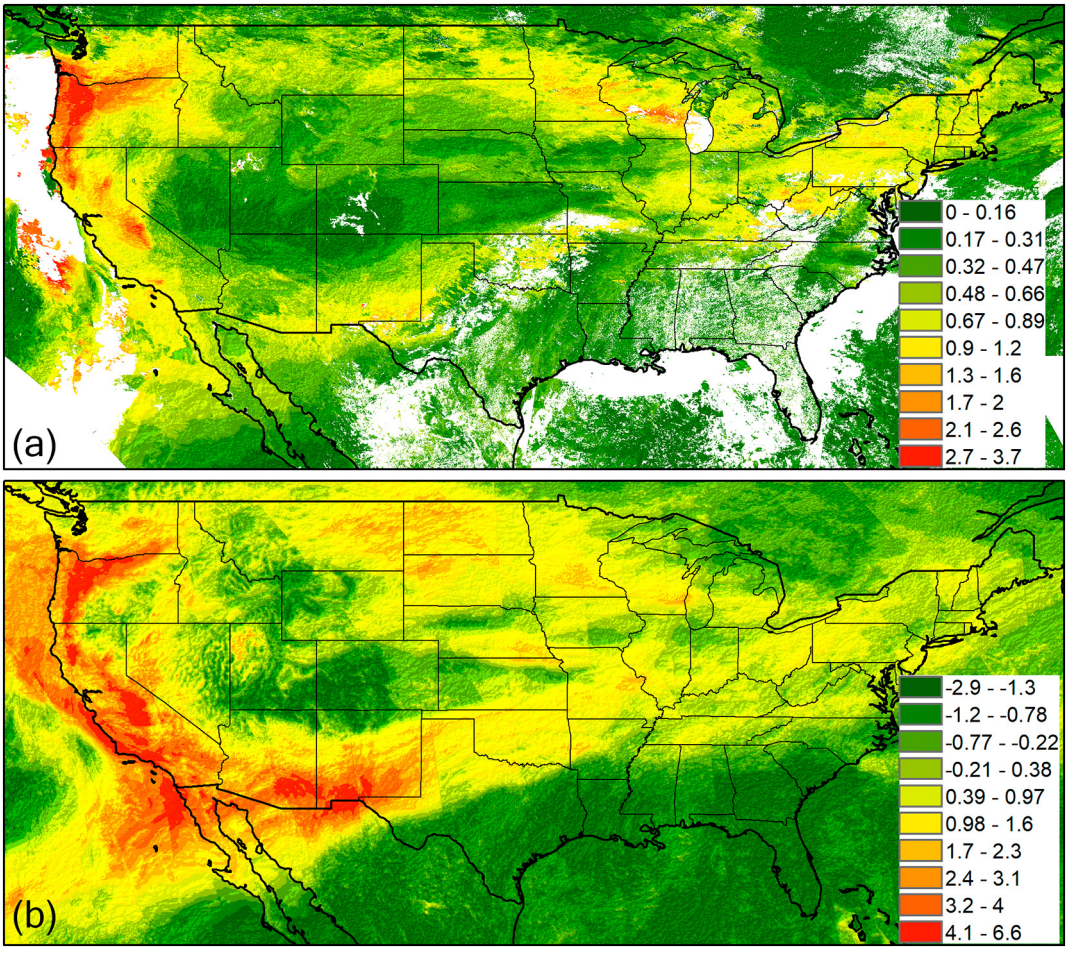

Fig. 6. Spatial distribution of **(a)** aerosol optical depth (AOD) obtained from MODIS MAIAC and **(b)** ultraviolet aerosol index (UVAI) obtained from TROPOMI over the US from 10 to 16 September 2020.

contribute to vertical air diffusion. As a result, this led to the movement of smog in the planetary air current system far beyond its formation, resulting in high AOD and UVAI values even in the east coast of the country.

Some studies have shown that smoke plumes from forest fires often do not extend beyond the boundary layer (Trentmann et al., 2002). However, large fires can release enough energy (see Fig. 4) to cause smoke to rise above the boundary layer. In this case, the smoke particles were found to extend from the ABL to the free troposphere (FT) (see Fig. S3). The mechanism of this development can be explained by a combination of several factors, it is the continuous emission of smoke from the surface in the ABL. These factors may contribute to the long transport of smog by easterly winds in the free troposphere.

A high and positive UVAI may be an indicator of mineral dust or smoke aerosols and can only be confirmed by using observations related to particle size. Therefore, Angstrom exponent (AE) and fine mode fraction (FMF) were used to study particle sizes using AERONET sun/sky radiometer measurements from NASA Ames (N37.420° W122.06°), Fresno 2 (N36.785° W119.773°) and the Mount Wilson (N34.225° W118.056°) located near the fire sources. In this study, AERONET Version 2, Level 2.0 data retrieval was used.

The AOD values obtained from the AERONET stations are in good agreement with the data from MODIS MAIAC. As can be seen from Table 1, the FMF ranged from 0.9 to almost 1, clearly indicating the predominance of smog layers in the atmosphere. Accordingly, AOD_c associated with coarse-mode was almost zero, and the total AOD (tAOD) was almost equal to the AOD_f of the fine-mode. This indicates that large particles were practically absent during this period. The Angstrom Exponent (AE) was mainly in the range of 1.2–1.5, again indicating the presence of a pronounced mode of accumulation of fine particles.

3.4. Vertical distribution aerosols and surface black carbon concentration

The main mechanism for the transfer of pollution from the local to the regional scale is the vertical transfer from the surface layer upward into the free troposphere, and from there it is carried by winds to other regions. The spread of smoke and dust plumes into the atmosphere facilitates the transfer of pollutants further from emission sources. To study the prevailing types of aerosols and their vertical distribution during the period of fire activity, data on their vertical profile obtained from CALIPSO lidar were used. CALIPSO Level 2 Version 4.21 cloud and quality screened data generated the aerosol classification and vertical aerosol extinction. Fig. 7 shows the day and night CALIPSO aerosol profiles obtained from September 10 to 15. The trajectories were chosen to cover the western and central parts of the country.

CALIPSO satellite trajectories over desert regions of the US, in vertical aerosol profile, showed dust layers at an altitude of 0 to 8 km (Fig. 7b, c, e, f, g, and h) in the central, western and southern regions of the country, including over dust sources in the Great Basin, Mojave Desert, Chihuahuan Desert, Sonoran Desert, Colorado Plateau, and Great Plains. Nevertheless, all profiles show dense layers of smog and polluted dust aerosols in the entire vertical profile (between 35 and 47°N) as a result of the intensive combustion of biomass. The range of extinction values over most of the territory was in the range from 0.15 to 1.2 km^{-1} at an altitude of up to 10 km from the surface (Fig. 8). High extinction values (>0.5 km^{-1}) can be attributed to smoke (biomass-related) and contaminated dust (a mixture of dust and biomass smoke), which is evident from the aerosol type classification. Aerosols, identified as smog, were also recorded between 20 and 30°N over the Pacific Ocean, Gulf of California, and Mexico, demonstrating that smoke aerosols could also move to the south and west.

During MERRA-2 reanalysis, black carbon surface mass concentration data were used, provided by NASA Global Modeling and Assimilation Office (GMAO) (Fig. 9). Large quantities of carbonaceous aerosols were released into the atmosphere during the wildfires. According to the figure, it was found that wildfires generated a large number of BC aerosols with a maximum surface mass concentration of approximately 370 $\mu g/m^3$, subsequently affecting the air quality far from the place of their formation (Shikwambana, 2019). The results of MERRA-2 reanalysis showed that the concentration of BC is similar to observations obtained by CALIPSO, indicating the presence of smog over the study area. Fig. 9 shows that smoke and polluted dust aerosols spread not only across the country but also covered the coastal waters, extending far into the ocean. At the same time, the concentration of BC is similar to that of AOD and UVAI. Chemically, BC is a component of $PM_{2.5}$, so it is not surprising that the spatial distribution and concentrations of BC and $PM_{2.5}$ are similar. These results are supported by results from other studies indicating that wildfires release a large amount of BC aerosols (Smirnov et al., 2015; Zhu et al., 2019; Biswas et al., 2020; Pandey et al., 2020; Nguyen et al., 2021).

4. Conclusions

In mid-August 2020, large wildfires erupted in the western part of the US, peaking between September 10–16, when smoke from the wildfires spread across most of the country. Wildfires occur annually in the region but are rarely so widespread. They destroy natural forest communities and contribute to the release of large amounts of combustion products

Table 1
Daily values of aerosol parameters derived from AERONET sky radiometer measurements.

AERONET site	Date	AOD_{500}	$tAOD_{500}$	AOD_f	AOD_c	$AE_{440–870}$	FMF_{500}
	10 Sep. 2020	5.608	–	–	–	1.506	–
	11 Sep. 2020	2.534	3.140	3.120	0.020	1.272	0.993
	12 Sep. 2020	0.859	1.199	1.181	0.018	1.252	0.984
NASA Ames	13 Sep. 2020	1.014	1.521	1.495	0.027	1.285	0.982
	14 Sep. 2020	0.646	0.828	0.800	0.028	0.896	0.966
	15 Sep. 2020	0.553	0.797	0.786	0.011	1.311	0.986
	16 Sep. 2020	0.125	0.187	0.180	0.006	1.395	0.964
	10 Sep. 2020	2.448	3.386	3.353	0.033	1.311	0.990
	11 Sep. 2020	3.600	4.737	4.716	0.021	1.331	0.996
	12 Sep. 2020	2.216	3.031	2.992	0.039	1.379	0.987
Fresno 2	13 Sep. 2020	1.646	2.190	2.165	0.025	1.315	0.988
	14 Sep. 2020	1.212	1.665	1.644	0.021	1.409	0.987
	15 Sep. 2020	1.166	1.670	1.645	0.025	1.367	0.985
	16 Sep. 2020	0.988	1.451	1.431	0.020	1.349	0.986
	10 Sep. 2020	2.814	4.140	4.088	0.052	1.343	0.988
	11 Sep. 2020	2.767	–	–	–	1.996	–
	12 Sep. 2020	2.326	3.014	2.957	0.057	1.215	0.982
Mount Wilson	13 Sep. 2020	0.460	0.701	0.676	0.025	1.264	0.963
	14 Sep. 2020	0.399	0.508	0.480	0.028	1.384	0.946
	15 Sep. 2020	0.909	1.299	1.204	0.095	1.452	0.937
	16 Sep. 2020	1.093	0.724	0.686	0.038	1.494	0.955

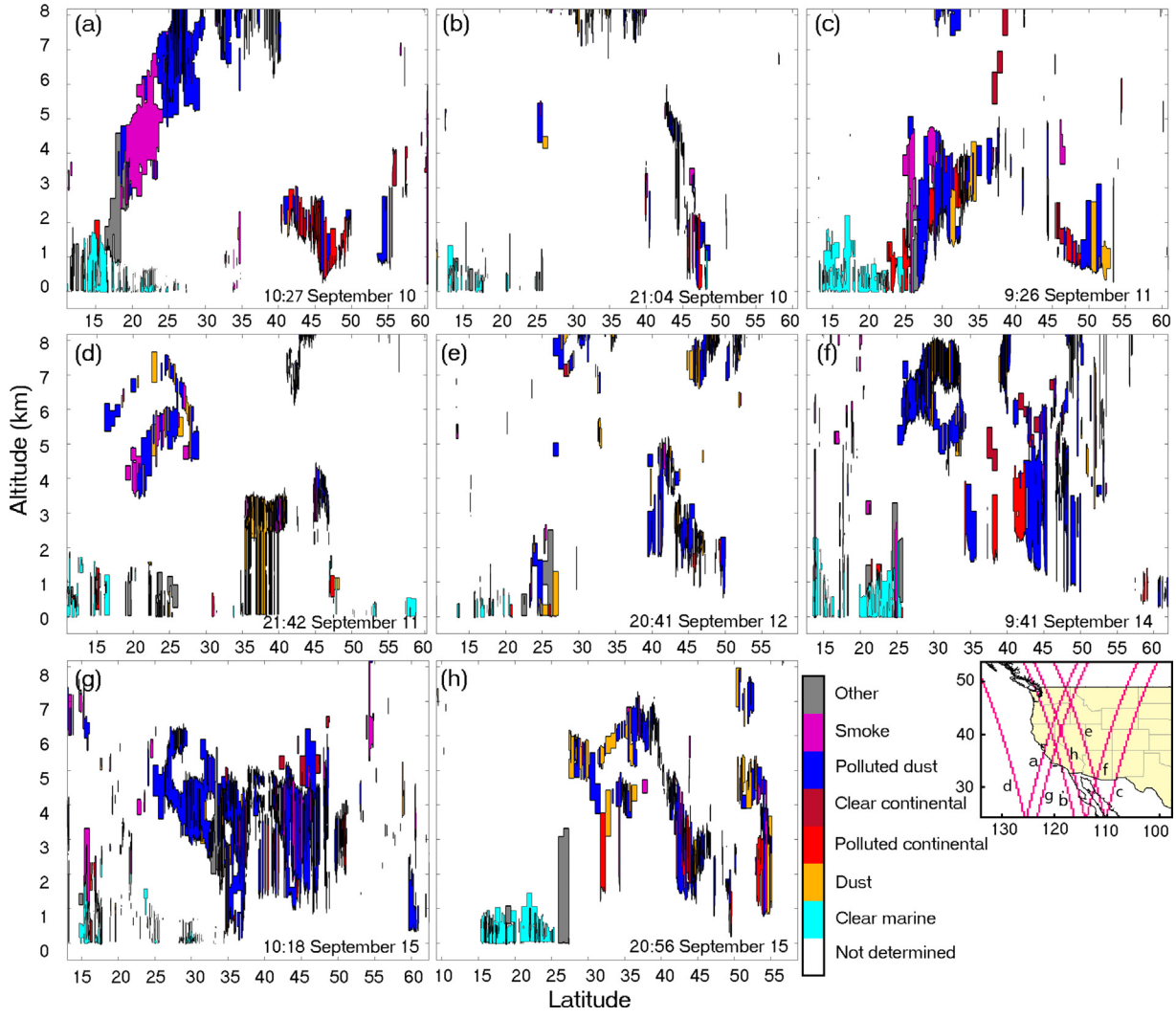

Fig. 7. CALIPSO Vertical Feature Mask (VFM) level 2 version 4.21 over the west and center of the US.

into the atmosphere, including small particles as measured by $PM_{2.5}$ and BC, that have serious environmental and health consequences.

This study quantified the impact of wildfires on air pollution in the affected areas using surface $PM_{2.5}$ concentrations and aerosol properties derived from satellite and reanalysis data. During the period of the greatest wildfire activity, September 10 to September 16, significant changes in the composition of the atmosphere in the region were observed, as evidenced from data of the TROPOMI and MODIS instruments. The most noticeable

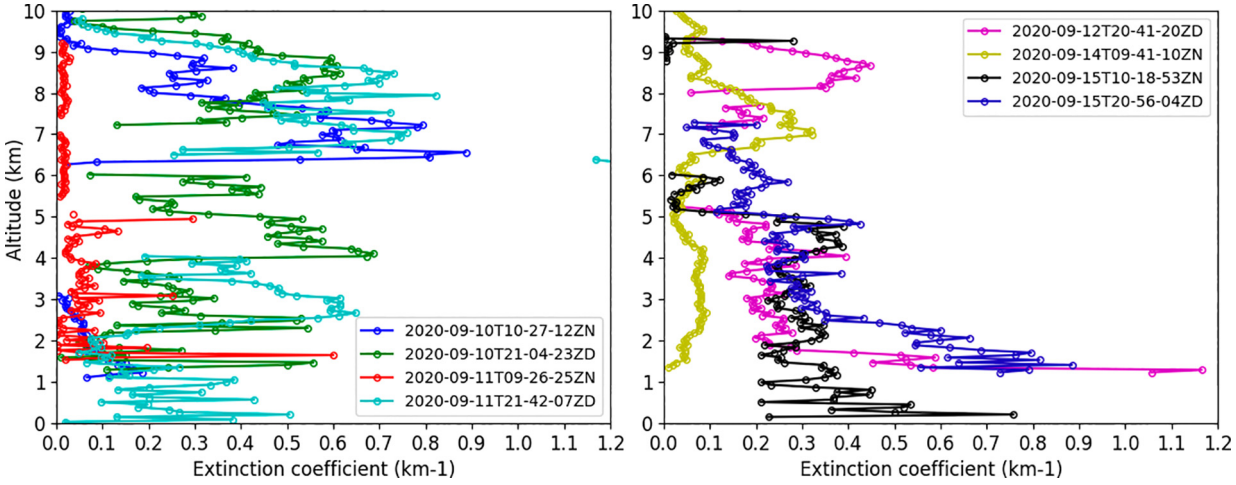

Fig. 8. CALIPSO Level 2 version 4.21 aerosol extinction coefficient (at 532 nm) vertical profile. The extinction profile is averaged for the region between 35 and 47°N latitude.

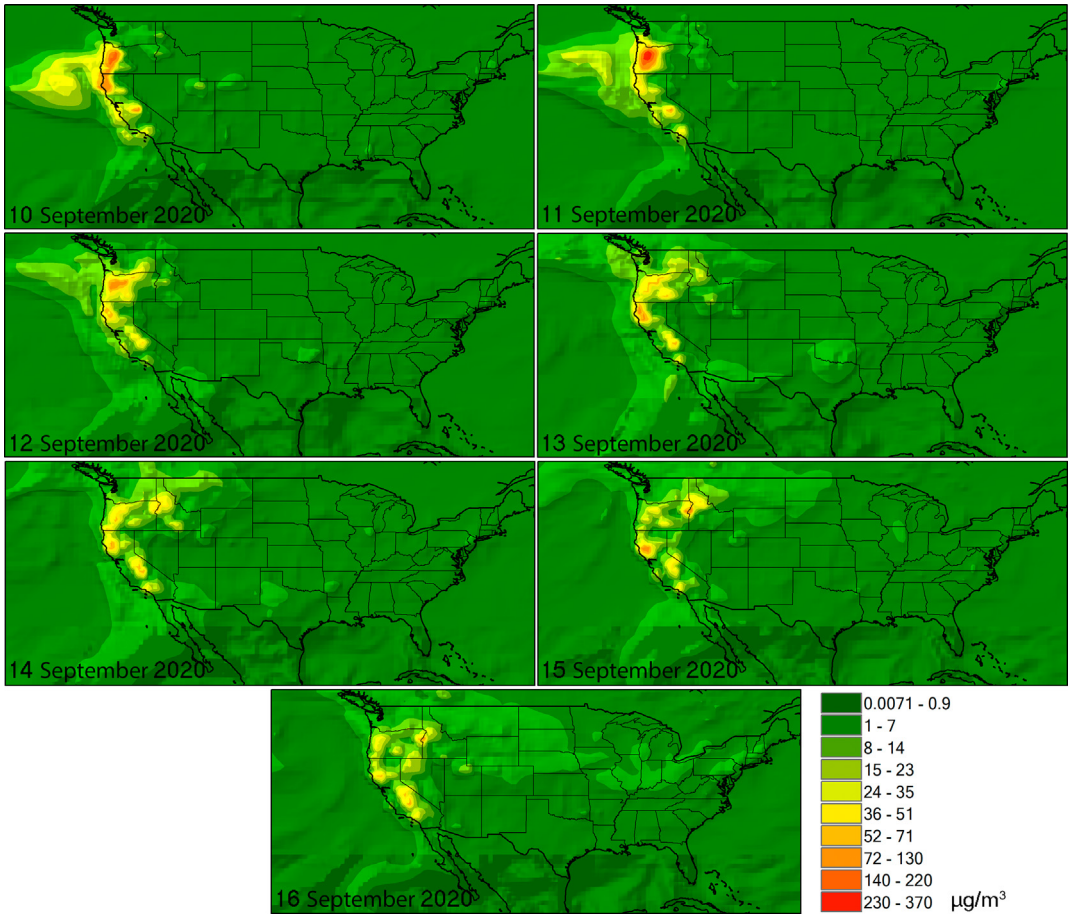

Fig. 9. Spatial distribution of MERRA-2 black carbon surface mass concentration (μg/m^3) over the US during 10–16 September 2020.

increase were in $PM_{2.5}$ concentrations that were several times higher than the established NAAQS limit. Aerosol loadings in the region grew at unprecendented rates with values of AOD and UVAI exceeding 1 and 2 for most of the country. In some areas of California, Oregon and Washington, these values reached 3.7 and 6.6, respectively.

Although wildfires are often episodic and of short duration, the high frequency and increased duration in recent years have made a long-term impact on people's lives. The results show a significant increase in pollution in western parts of the country within a short period, affecting millions of people. Other parts of the country are also negatively affected. Due to the increase in the number of wildfires in recent years, more research is needed on the long-range transport of smoke from wildfires and its effect on human health.

In the future, as climate change accelerates, leading to higher temperatures and possible drought, wildfires are likely to become more frequent and intense, with greater impacts on air quality in areas near and far. Research can help identify the increase in the concentration of air pollutants that result from such wildfires. Since the ground air quality monitoring network is sparse, satellite observations will play an important role. Further work is also needed to assess the associated health risks of air pollutants from wildfires. Results of this research can be used for a comprehensive analysis of the state of the atmosphere at the time of wildfires and for assessing the nature and volume of gas emissions into the atmosphere.

CRediT authorship contribution statement

Mikalai Filonchyk: Methodology, Formal analysis, Investigation, Writing – original draft, Visualization. **Michael P. Peterson:** Writing – review & editing, Methodology, Formal analysis. **Dongqi Sun:** Writing – review & editing.

Declaration of competing interest

The authors declared that they have no conflict of interests.

Acknowledgements

The work was financially supported by the Open Fund of Key Laboratory of Urban Land Resources Monitoring and Simulation, Ministry of Natural Resource (KF-2020-05-067), and key research project supported by Gansu Natural Science Foundation (21JR7RA281, 21JR7RA278).

Appendix A. Supplementary data

Supplementary data to this article can be found online at https://doi.org/10.1016/j.scitotenv.2022.154103.

References

Akinwumiju, A.S., Ajisafe, T., Adelodun, A.A., 2021. Airborne particulate matter pollution in Akure Metro City, southwestern Nigeria, West Africa: attribution and meteorological influence. J. Geovis. Spat. Anal. 5 (1), 1–17.

Avissar, R., Silva Dias, P.L., Silva Dias, M.A., Nobre, C., 2002. The large-scale biosphere-atmosphere experiment in Amazonia (LBA): insights and future research needs. J. Geophys. Res. Atmos. 107 (D20), LBA-54.

Biswas, K., Chatterjee, A., Chakraborty, J., 2020. Comparison of air pollutants between Kolkata and Siliguri, India, and its relationship to temperature change. J. Geovis. Spat. Anal. 4 (2), 1–15.

Chen, C., Cai, J., Wang, C., Shi, J., Chen, R., Yang, C., Kan, H., 2018. Estimation of personal PM2. 5 and BC exposure by a modeling approach–results of a panel study in Shanghai, China. Environ. Int. 118, 194–202.

Columbia Broadcasting System (CBS), 2020. Wildfire photos and videos show "apocalyptic" red and orange skies across Western U.S. https://www.cbsnews.com/news/wildfire-sky-orange-bay-area-california-western-united-states/. (Accessed 9 October 2020).

Dias, M.S., Rutledge, S., Kabat, P., Dias, P.S., Nobre, C., Fisch, G., Gatti, L., 2002. Cloud and rain processes in a biosphere-atmosphere interaction context in the Amazon region. J. Geophys. Res. Atmos. 107 (D20), LBA-39.
ECMWF, 2018. What are the differences changes from ERA-Interim to ERA5? https://confluence.ecmwf.int//pages/viewpage.action?pageId=74764925
Filonchyk, M., Peterson, M., 2020. Air quality changes in Shanghai, China, and the surrounding urban agglomeration during the COVID-19 lockdown. J. Geovis. Spat. Anal. 4 (2), 1–7.
Freeborn, P.H., Wooster, M.J., Hao, W.M., Ryan, C.A., Nordgren, B.L., Baker, S.P., Ichoku, C., 2008. Relationships between energy release, fuel mass loss, and trace gas and aerosol emissions during laboratory biomass fires. J. Geophys. Res. Atmos. 113, D1301.
Gelaro, R., McCarty, W., Suárez, M.J., Todling, R., Molod, A., Takacs, L., Zhao, B., 2017. The modern-era retrospective analysis for research and applications, version 2 (MERRA-2). J. Clim. 30 (14), 5419–5454.
Gorchakov, G.I., Sitnov, S.A., Sviridenkov, M.A., Semoutnikova, E.G., Emilenko, A.S., Isakov, A.A., Ponomareva, T.Y., 2014. Satellite and ground-based monitoring of smoke in the atmosphere during the summer wildfires in European Russia in 2010 and Siberia in 2012. Int. J. Remote Sens. 35 (15), 5698–5721.
Gustafsson, Ö., Ramanathan, V., 2016. Convergence on climate warming by black carbon aerosols. Proc. Natl. Acad. Sci. U. S. A. 113 (16), 4243–4245.
Huang, S., Liu, H., Dahal, D., Jin, S., Li, S., Liu, S., 2016. Spatial variations in immediate greenhouse gases and aerosol emissions and resulting radiative forcing from wildfires in interior Alaska. Theor. Appl. Climatol. 123 (3–4), 581–592.
Hung, W.T., Lu, C.H.S., Alessandrini, S., Kumar, R., Lin, C.A., 2021. The impacts of transported wildfire smoke aerosols on surface air quality in New York State: a multi-year study using machine learning. Atmos. Environ. 118513.
Jiang, Y., Zhuang, Q., 2011. Extreme value analysis of wildfires in Canadian boreal forest ecosystems. Can. J. For. Res. 41 (9), 1836–1851.
Justice, C.O., Giglio, L., Korontzi, S., Owens, J., Morisette, J.T., Roy, D., Kaufman, Y., 2002. The MODIS fire products. Remote Sens. Environ. 83 (1–2), 244–262.
Kawai, K., Kai, K., Jin, Y., Sugimoto, N., Batdorj, D., 2018. Lidar network observation of dust layer development over the Gobi Desert in association with a cold frontal system on 22–23 may 2013. J. Meteor. Soc. Jpn. 96 (3), 255–268.
Keeley, J.E., Syphard, A.D., 2021. Large California wildfires: 2020 fires in historical context. Fire Ecol. 17 (1), 1–11.
Khain, A.P., BenMoshe, N., Pokrovsky, A., 2008. Factors determining the impact of aerosols on surface precipitation from clouds: an attempt at classification. J. Atmos. Sci. 65 (6), 1721–1748.
Kumari, P., Toshniwal, D., 2020. Impact of lockdown on air quality over major cities across the globe during COVID-19 pandemic. Urban Clim. 34, 100719.
Leng, C., Zhang, Q., Zhang, D., Xu, C., Cheng, T., Zhang, R., Gao, W., 2014. Variations of cloud condensation nuclei (CCN) and aerosol activity during fog–haze episode: a case study from Shanghai. Atmos. Chem. Phys. 14 (22), 12499–12512.
Li, F., Zhang, X., Kondragunta, S., Lu, X., 2020a. An evaluation of advanced baseline imager fire radiative power based wildfire emissions using carbon monoxide observed by the tropospheric monitoring instrument across the conterminous United States. Environ. Res. Lett. 15 (9), 094049.
Li, L., Girguis, M., Lurmann, F., Pavlovic, N., McClure, C., Franklin, M., Habre, R., 2020b. Ensemble-based deep learning for estimating PM2.5 over California with multisource big data including wildfire smoke. Environ. Int. 145, 106143.
Liu, J., Li, Z., Zheng, Y., Chiu, J.C., Zhao, F., Cadeddu, M., Cribb, M., 2013. Cloud optical and microphysical properties derived from ground-based and satellite sensors over a site in the Yangtze Delta region. J. Geophys. Res. Atmos. 118 (16), 9141–9152.
Liu, Z., Kuehn, R., Vaughan, M., Winker, D., Omar, A., Powell, K., Trepte, C., Hu, Y., Hostetler, C., 2010. The CALIPSO cloud and aerosol discrimination: version 3 algorithm and test results. 25th International Laser Radar Conference (ILRC), St. Petersburg, Russia, pp. 5–9.
Louie, D., 2020. October 10). Damage from California's wildfires estimated at $10 billion, experts say. ABC 7 News. https://abc7news.com/california-wildfires-cost-of-cal-fire-stanford-wildfire-research/6897462/
Lyapustin, A., Wang, Y., Korkin, S., Huang, D., 2018. MODIS collection 6 MAIAC algorithm. Atmos. Meas. Tech. 11 (10), 5741–5765.
Martins, J.A., Dias, M.S., 2009. The impact of smoke from forest fires on the spectral dispersion of cloud droplet size distributions in the amazonian region. Environ. Res. Lett. 4 (1), 015002.
Menut, L., Bessagnet, B., Siour, G., Mailler, S., Pennel, R., Cholakian, A., 2020. Impact of lockdown measures to combat Covid-19 on air quality over western Europe. Sci. Total Environ. 741, 140426.
Meyer, K., Platnick, S., Zhang, Z., 2015. Simultaneously inferring above-cloud absorbing aerosol optical thickness and underlying liquid phase cloud optical and microphysical properties using MODIS. J. Geophys. Res. Atmos. 120 (11), 5524–5547.
Mota, B., Wooster, M.J., 2018. A new top-down approach for directly estimating biomass burning emissions and fuel consumption rates and totals from geostationary satellite fire radiative power (FRP). Remote Sens. Environ. 206, 45–62.
Mozny, M., Trnka, M., Brázdil, R., 2021. Climate change driven changes of vegetation fires in the Czech Republic. Theor. Appl. Climatol. 143 (1), 691–699.
Naqvi, H.R., Datta, M., Mutreja, G., Siddiqui, M.A., Naqvi, D.F., Naqvi, A.R., 2021. Improved air quality and associated mortalities in India under COVID-19 lockdown. Environ. Pollut. 268, 115691.
Nguyen, H.D., Azzi, M., White, S., Salter, D., Trieu, T., Morgan, G., Nguyen, H., 2021. The summer 2019–2020 wildfires in East Coast Australia and their impacts on air quality and health in New South Wales, Australia. Int. J. Environ. Res. Public Health 18 (7), 3538.
Nikhil, S., Danumah, J.H., Saha, S., Prasad, M.K., Rajaneesh, A., Mammen, P.C., Kuriakose, S.L., 2021. Application of GIS and AHP method in forest fire risk zone mapping: a study of the Parambikulam Tiger Reserve, Kerala, India. J. Geovis. Spat. Anal. 5 (1), 1–14.
Pandey, C.P., Singh, J., Soni, V.K., Singh, N., 2020. Yearlong first measurements of black carbon in the western Indian Himalaya: influences of meteorology and fire emissions. Atmos. Pollut. Res. 11 (7), 1199–1210.
Raffuse, S.M., McCarthy, M.C., Craig, K.J., DeWinter, J.L., Jumbam, L.K., Fruin, S., Lurmann, F.W., 2013. High-resolution MODIS aerosol retrieval during wildfire events in California for use in exposure assessment. J. Geophys. Res. Atmos. 118 (19), 11–242.
Rakhimov, R.F., Kozlov, V.S., Panchenko, M.V., Tumakov, A.G., Shmargunov, V.P., 2014. Properties of atmospheric aerosol in smoke plumes from forest fires according to spectronephelometer measurements. Atmos. Ocean. Opt. 27 (3), 275–282.
Shikwambana, L., 2019. Long-term observation of global black carbon, organic carbon and smoke using CALIPSO and MERRA-2 data. Remote Sens. Lett. 10 (4), 373–380.
Smirnov, N.S., Korotkov, V.N., Romanovskaya, A.A., 2015. Black carbon emissions from wildfires on forest lands of the Russian Federation in 2007–2012. Russ. Meteorol. Hydrol. 40 (7), 435–442.
Tian, X.R., Shu, L.F., Zhao, F.J., Wang, M.Y., McRae, D.J., 2011. Future impacts of climate change on forest fire danger in northeastern China. J. For. Res. 22 (3), 437–446.
Trentmann, J., Andreae, M.O., Graf, H.F., Hobbs, P.V., Ottmar, R.D., Trautmann, T., 2002. Simulation of a biomass-burning plume: comparison of model results with observations. J. Geophys. Res. Atmos. 107 (D2), AAC-5.
Uzan, L., Egert, S., Alpert, P., 2016. Ceilometer evaluation of the eastern Mediterranean summer boundary layer height–first study of two Israeli sites. Atmos. Meas. Tech. 9 (9), 4387–4398.
Veefkind, J.P., Aben, I., McMullan, K., Förster, H., De Vries, J., Otter, G., Levelt, P.F., 2012. TROPOMI on the ESA Sentinel-5 precursor: a GMES mission for global observations of the atmospheric composition for climate, air quality and ozone layer applications. Remote Sens. Environ. 120, 70–83.
Wang, Q., Zhong, M., Wang, S., 2012. A meta-analysis on the response of microbial biomass, dissolved organic matter, respiration, and N mineralization in mineral soil to fire in forest ecosystems. For. Ecol. Manag. 271, 91–97.
Westervelt, D.M., Horowitz, L.W., Naik, V., Tai, A.P.K., Fiore, A.M., Mauzerall, D.L., 2016. Quantifying PM2.5-meteorology sensitivities in a global climate model. Atmos. Environ. 142, 43–56.
Wooster, M.J., Roberts, G., Perry, G.L.W., Kaufman, Y.J., 2005. Retrieval of biomass combustion rates and totals from fire radiative power observations: FRP derivation and calibration relationships between biomass consumption and fire radiative energy release. J. Geophys. Res. Atmos. 110, D24311.
World Health Organization (WHO), 2005. WHO Air Quality Guidelines for Particulate Matter, Ozone, Nitrogen Dioxide and Sulfur Dioxide. Global Update. Summary of Risk Assessment. Author, Geneva, Switzerland.
Wotton, B.M., Flannigan, M.D., Marshall, G.A., 2017. Potential climate change impacts on fire intensity and key wildfire suppression thresholds in Canada. Environ. Res. Lett. 12 (9), 095003.
Wyche, K.P., Nichols, M., Parfitt, H., Beckett, P., Gregg, D.J., Smallbone, K.L., Monks, P.S., 2021. Changes in ambient air quality and atmospheric composition and reactivity in the south east of the UK as a result of the COVID-19 lockdown. Sci. Total Environ. 755, 142526.
Zhang, X., Gui, K., Liao, T., Li, Y., Wang, X., Zhang, X., Xu, J., 2021. Three-dimensional spatiotemporal evolution of wildfire-induced smoke aerosols: A case study from Liangshan, Southwest China. Sci. Total Environ. 762, 144586.
Zhou, L., Dang, X., Mu, H., Wang, B., Wang, S., 2021. Cities are going uphill: slope gradient analysis of urban expansion and its driving factors in China. Sci. Total Environ. 775, 145836.
Zhou, L., Yuan, B., Mu, H., Dang, X., Wang, S., 2021. Coupling relationship between construction land expansion and PM 2.5 in China. Environ. Sci. Pollut. Res. 22, 33669–33681.
Zhu, C., Kanaya, Y., Yoshikawa-Inoue, H., Irino, T., Seki, O., Tohjima, Y., 2019. Sources of atmospheric black carbon and related carbonaceous components at Rishiri Island, Japan: the roles of Siberian wildfires and of crop residue burning in China. Environ. Pollut. 247, 55–63.
Zhu, Y., Xie, J., Huang, F., Cao, L., 2020. The mediating effect of air quality on the association between human mobility and COVID-19 infection in China. Environ. Res. 189, 109911.